# Spin coating of an evaporating polymer solution

Andreas Münch,[1,a)] Colin P. Please,[2,b)] and Barbara Wagner[3,c)]
[1]*Mathematical Institute, University of Oxford, 24-29 St. Giles', Oxford OX1 3LB, United Kingdom*
[2]*School of Mathematics, University of Southampton, University Road, Southampton SO17 1BJ, United Kingdom*
[3]*Department of Mathematics, Technische Universität Berlin, Straße des 17. Juni 136, 10623 Berlin, Germany*

(Received 4 October 2010; accepted 7 September 2011; published online 4 October 2011)

We consider a mathematical model of spin coating of a single polymer blended in a solvent. The model describes the one-dimensional development of a thin layer of the mixture as the layer thins due to flow created by a balance of viscous forces and centrifugal forces and evaporation of the solvent. In the model both the diffusivity of the solvent in the polymer and the viscosity of the mixture are very rapidly varying functions of the solvent mass fraction. Guided by numerical solutions an asymptotic analysis reveals a number of different possible behaviours of the thinning layer dependent on the nondimensional parameters describing the system. The main practical interest is in controlling the appearance and development of a "skin" on the polymer where the solvent concentration reduces rapidly on the outer surface leaving the bulk of the layer still with high concentrations of solvent. In practice, a fast and uniform drying of the film is required. The critical parameters controlling this behaviour are found to be the ratio of the diffusion to advection time scales $\epsilon$, the ratio of the evaporation to advection time scales $\delta$ and the ratio of the diffusivity of the pure polymer and the initial mixture $\exp(-1/\gamma)$. In particular, our analysis shows that for very small evaporation with $\delta \ll \exp(-3/(4\gamma))\epsilon^{3/4}$ skin formation can be prevented. © *2011 American Institute of Physics*. [doi:10.1063/1.3643692]

## I. INTRODUCTION

Spin coating of polymers blended in volatile solvents is one of the most widespread methods used in the coating industry to produce a uniformly thin surface of as little as a few hundred nanometre thickness. It is used for many technologies including the production of electronic devices[1] or organic solar cells.[2,3]

Theoretical studies on thinning rates and morphological evolution of a spin coated film go back to Emslie *et al.*,[4] who considered the simplest case of a single-component, non-volatile Newtonian liquid. It was followed by studies on the spreading rate of the thin film and its stability properties.[5–10] Further aspects, such as non-Newtonian rheology and colloidal suspensions or thermal effects were later also included.[11–17] The important effects of a volatile component added to the liquid, was first investigated experimentally by Kreith *et al.*[18] More recent experimental results can be found for example in Birnie and Manley.[19] The first theoretical treatment of spin coating an evaporating solution is due to Meyerhofer[20] and was later extended by Sukanek,[21] Bornside *et al.*,[22] and Reisfeld *et al.*[23,24] Additional effects if a volatile component is added, such as variable viscosity and diffusion coefficients during the thinning of the film and its effects on the stability of the film, have also been intensely studied asymptotically and numerically during the past decade.[25–31] One important feature that occurs due to the evaporation of the volatile component is the phenomenon of "skin" formation. This has first been studied by Lawrence,[32,33] see also de Gennes[34] and Okuzono *et al.*[35] for further discussions on this aspect. As discussed by Bornside *et al.*,[22] the phenomenon of skin formation is accompanied by a high viscosity and low solvent diffusivity at the free surface and is undesired in practical applications, since it may lead to coating defects. To our knowledge, the precise theoretical characterisation of skin formation is not available and the interplay of the many time and spatial scales involved in the evaporative spin coating process have not been completely quantified, even for the spin coating problem of a solution of a single polymer blended in a single volatile solvent and is the focus of this study.

We base our study on the situation and experimental data given in Bornside *et al.*[22] and Meyerhofer.[20] Their model assumes an exponential dependence of the solvent diffusivity on the concentration and an algebraic dependence of the liquid viscosity. This process has several time scales. Roughly speaking, there is a very fast initial time scale lasting only a few seconds which is dominated by convection of fluid in radial direction accompanied by very fast thinning and negligible evaporation. Subsequently, on a longer time scale convection becomes negligible and the process is dominated by evaporation of the solvent controlled by diffusion. There are further longer time scales that lead eventually to formation of a "skin". However, for more volatile solvents or larger initial mass fraction of the polymer, skin formation may occur on a much shorter time scale.

Our aim is to quantify in which parameter regimes which behaviour will occur and present a systematic approach using matched asymptotic expansions in order to quantitatively

a)Electronic mail: muench@maths.ox.ac.uk.
b)Electronic mail: c.p.please@soton.ac.uk.
c)Electronic mail: bwagner@math.tu-berlin.de.

 

characterise the various processes. In this study, we restrict ourselves to a simplified one-dimensional model assuming a exponential dependence for both the diffusivity and viscosity on the solvent concentration and moreover assume a Newtonian rheology, to lay a foundation for the systematic asymptotic study of the film behaviour. Moreover, we note that in this paper we assume that the film can be brought into a uniform state from the beginning, i.e., the initial distribution is independent of the lateral position. Under this assumption, our asymptotic analysis is able to determine the various parameter regimes, in particular when skin formation occurs and on what time scale. We compare our analytic solutions to those of our numerical code that uses nonuniform grids in order to capture the self-similar approach toward blow-up in our mathematical model, i.e., skin formation. If the initial liquid distribution is not uniform, the theory still applies to the later times regimes if the evaporation is not too large.

Extensions of our present analysis that include more realistic constitutive laws for the concentration dependence of the viscosity as well as non-Newtonian rheologies and the effect of extensional stresses in the surface layer will likely give rise to a richer asymptotic picture. Details regarding the validity will be discussed further in the conclusions after we have developed our theory.

## II. GENERAL BEHAVIOUR OF A SPIN COATED LAYER

From the detailed analysis of the model presented in this paper we have found that in most physically relevant circumstances there are a number of different behaviours that can occur. In examining these we consider the physically relevant case where changes in diffusion coefficient due to changes in solvent concentration occur on the same scale as the changes in the viscosity. These behaviours are dependent primarily on the relative importance of three time scales in the problem and the initial volume ratio of polymer to solvent. The three timescales are (i) the diffusion time of the solvent across the initial layer, (ii) the time to advect across the initial layer due to the vertical velocity induced by the centrifugal and viscous forces, and (iii) the time to evaporate solvent from the initial layer. The relative size of these time scales is readily captured by considering the parameters $\epsilon$, the ratio of the diffusion to advection time scales and $\delta$, the ratio of the evaporation to advection time scales, both of which are very small in any practical situation, and $\gamma$, where $\exp(-1/\gamma)$ is the ratio of the solvent diffusivity in the pure polymer and that in the polymer/solvent mixture at $t=0$. Our analysis shows that there are three main regimes of behaviour corresponding to

(i) $\delta \ll \epsilon^{3/4} \ll 1$ (small evaporation)
(ii) $\epsilon^{3/4} \ll \delta \ll \epsilon^{1/2} \ll 1$ (medium evaporation)
(iii) $\epsilon^{1/2} \ll \delta \ll 1$ (large evaporation).

In each case, the balance of mechanisms governing the development of the layer changes as time progresses. Most interestingly, the case (i) has a limiting case

(ia) $\delta \ll \exp(-3/(4\gamma))\epsilon^{3/4}$ (very small evaporation),

where, unlike in the other cases, there is no skin formation. To illustrate this situation, we show in Figure 1 how the $\epsilon - \delta$ parameter space subdivides into these different asymptotic regimes for $\epsilon \ll 1$ and $\delta \ll 1$.

The figure shows how the $\epsilon - \delta$ parameter space subdivides into four different asymptotic regimes as for $\epsilon \ll 1$ and $\delta \ll 1$.

In all cases initially the layer thins due to centrifugal forces balancing with viscous stresses while evaporation causes changes in solvent concentration in a narrow boundary layer near the surface. If the solvent mass fraction variations in this boundary layer become significant so that diffusion drops dramatically, a skin is formed. Once a skin has formed, there is a much longer time scale over which the mass fraction slowly equilibrates.

In the large evaporation case, the skin forms before the layer thins significantly; in the medium evaporation case, the skin forms after the layer has thinned. In both cases, when the thin skin forms, the material under the skin still has its initial consistency.

When the evaporation rate is small, a thin skin forms with the material underneath being spatially uniform but at a solvent concentration that is much less than its initial value. For the very small evaporation rate, no skin forms.

## III. BASIC ONE-DIMENSIONAL MODEL

We consider the movement of a mixture on a spinning disk which spins with angular velocity $\omega$ about the $z$ axis (hence, $\boldsymbol{\omega} = \omega z$). The coordinate system is fixed in the disk with $r$ as the radial distance and the mixture between the spinning disk $z=0$ and the upper surface $z=h(r,t)$. The mixture is taken to have a mass fraction of the volatile solvent $\phi(r,z,t)$ with the polymer having mass fraction $1-\phi$ $(r,z,t)$. We consider the mixture to flow radially symmetrically and act as an incompressible Newtonian fluid, with the fluid velocity being velocity $\boldsymbol{u}$ with components $u(r,z,t)$ in the radial

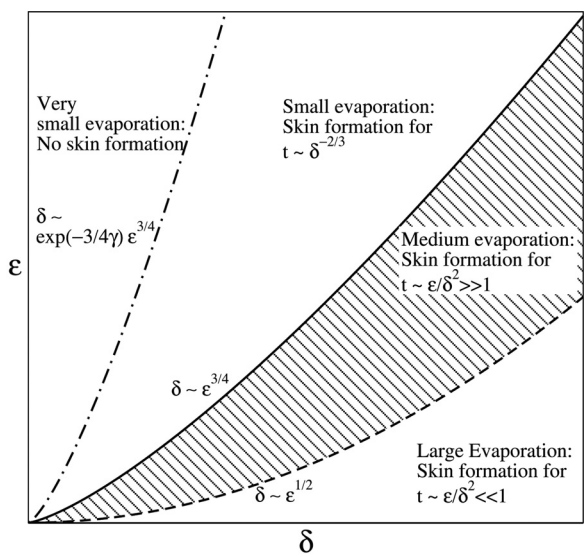


FIG. 1. Overview of the asymptotic regimes in the $\epsilon - \delta$ plane for small $\epsilon$ and $\delta$: We illustrate that skin formation should occur in all regimes except the one with the smallest evaporation, delimited by the dashed-dotted curve. Below this curve skin formation occurs on increasingly shorter time scales as we enter the asymptotic regimes separated by the solid and the dashed curves.

direction and $w(r,z,t)$ in the $z$ direction. We assume the viscosity $\eta(\phi)$ to be very strongly dependent on the solvent mass fraction, and that diffusion of the solvent through the mixture be represented by a diffusion coefficient $\mathcal{D}(\phi)$, which is also very strongly dependent on the solvent mass fraction. We assume the density of the mixture, $\rho$, is independent of the solvent mass fraction so that the governing equations are as follows:

The momentum equations are

$$\rho(\partial_t \boldsymbol{u} + \boldsymbol{u}\cdot\nabla\boldsymbol{u}) = \nabla\cdot\boldsymbol{T} - \rho[2\omega\times\boldsymbol{u} + \omega\times(\omega\times\boldsymbol{r})], \quad (1a)$$

where the stress tensor is given by $\boldsymbol{T} = -p\boldsymbol{I} + \eta(\phi)\,\dot{\gamma}$ with the strain rate $\dot{\gamma} = \nabla\boldsymbol{u} + (\nabla\boldsymbol{u})^T$ and $\boldsymbol{I}$ is the identity matrix. The continuity equation is given by

$$\nabla\cdot\boldsymbol{u} = 0. \quad (1b)$$

These are coupled to the diffusion equation for the solvent mass fraction,

$$\partial_t\phi + \boldsymbol{u}\cdot\nabla\phi = \nabla\cdot(\mathcal{D}(\phi)\nabla\phi), \quad (1c)$$

where we chose for simplicity,

$$\eta(\phi) = \eta_0\, e^{-\phi/2b} \quad \text{and} \quad \mathcal{D}(\phi) = D_0\, e^{\phi/2a}, \quad (1d)$$

for the functional dependency of the viscosity and diffusion on the mass fraction. The constants $\eta_0$, $D_0$, $a$, and $b$ are material constants. Note, that Bornside *et al.*[22] used this exponential to describe the diffusion coefficient but used an algebraic expression to describe the viscosity. We introduced the alternative fit for $\eta$ which matches the average variation of the viscosity in the experimental data as the mass fraction varies from zero to one, since having an exponential dependence of both $\eta$ and $D$ on $\phi$ facilitates the derivation of the asymptotic theory. However, the precise details of the dependency of the diffusion coefficient and the viscosity are not essential of the following discussions. Nevertheless, for a more realistic model it would be interesting to consider constitutive laws that allow for a more rapid change of viscosity with polymer concentration than of the solvent diffusivity. Also, we neglect non-Newtonian properties of polymer solutions and the relevance of extensional stresses in the polymer rich boundary layer on the flow.

For the boundary conditions at the free surface $z = h(r,t)$ we have the normal and tangential stress conditions. We assume that there is a surface tension, $\sigma$, acting and no tangential stress so that forms at the surface,

$$\boldsymbol{n}\cdot\boldsymbol{T}\cdot\boldsymbol{n} = \sigma\nabla\cdot\boldsymbol{n} \quad \text{and} \quad \boldsymbol{n}\cdot\boldsymbol{T}\cdot\boldsymbol{t} = 0\,. \quad (1e)$$

For the kinematic condition we have

$$\boldsymbol{u}\cdot\boldsymbol{n} - \frac{\partial_t h}{\sqrt{1+(\partial_r h)^2}} = \frac{J(\phi)}{\rho}, \quad (1f)$$

where $J(\phi)$ denotes the flux due to evaporation. Following Bornside *et al.*,[22] we approximate the mass flux of solvent from the liquid into the gas by

$$J(\phi) = k\,\rho\,\phi, \quad (1g)$$

with a mass transfer coefficient $k$ that is proportional to $\omega^{1/2}$ (to incorporate the effect of the gas flow above the disk, see also Bornside, Brown *et al.*[36]), where we also have assumed that the equilibrium solvent mass fraction is sufficiently small so that it can be set to zero.

Finally, conservation of solvent at this surface gives

$$-\mathcal{D}(\phi)\,\nabla\phi\cdot\boldsymbol{n} + \phi(\boldsymbol{u}\cdot\boldsymbol{n} - \frac{\partial_t h}{\sqrt{1+(\partial_r h)^2}}) = \frac{J(\phi)}{\rho}, \quad (1h)$$

or, using (1f)

$$\mathcal{D}(\phi)\,\nabla\phi\cdot\boldsymbol{n} = -\frac{J(\phi)}{\rho}(1-\phi). \quad (1i)$$

Boundary conditions at the solid substrate $z = 0$ are the no-slip and impermeability conditions,

$$\boldsymbol{u} = 0 \qquad \nabla\phi\cdot\boldsymbol{n} = 0. \quad (1j)$$

For the initial conditions we let

$$h(r,0) = h_{\text{in}} \quad \text{and} \quad \phi(r,z,0) = \phi_{\text{in}}\,. \quad (1k)$$

To analyse the problem we put it into nondimensional form and consider suitable limiting cases from the various parameters in the problem. Note, we non-dimensionalise the problem using the overbar notation for the nondimensional variables, but for simplicity of notation, we will immediately drop the overbar notation from thereon,

$$r = \mathbb{L}\bar{r}, \quad z = \mathbb{H}\bar{z}, \quad h = \mathbb{H}\bar{h}, \quad h_{\text{in}} = \mathbb{H}, \quad (2a)$$

$$u = \mathbb{U}\bar{u}, \quad w = \epsilon_\ell\mathbb{U}\bar{w}, \quad T = \frac{\mathbb{L}}{\mathbb{U}}\bar{t}, \quad (2b)$$

where we take the characteristic height $\mathbb{H}$ as the initial height $h_{\text{in}}$ of the layer, $\mathbb{L}$ as the radius of the spinning disk and introduce the aspect ratio $\epsilon_\ell = \mathbb{H}/\mathbb{L}$. For the characteristic velocity we choose

$$\mathbb{U} = \frac{2\rho\omega^2\mathbb{H}^2\mathbb{L}}{\eta_0 e^{-\phi_{\text{in}}/2b}}. \quad (2c)$$

For $\phi$ we let

$$\phi = \phi_{\text{in}} + 2a\bar{\phi}, \quad (2d)$$

so that

$$\eta = \eta_0 e^{-\phi_{\text{in}}/2b}\, e^{-\varrho\bar{\phi}} \quad \text{and} \quad \mathcal{D} = D_0\, e^{\phi_{\text{in}}/2a} e^{\bar{\phi}}, \quad (2e)$$

where $\varrho = a/b$. Notice that the scaling (2d) for the mass fraction has been chosen so that order one changes in $\bar{\phi}$ correspond to order one changes in the viscosity and diffusivity. Since the typical values for $a$ and $b$ are small (see Table I) this is not the case for the dependence of $\eta$ and $D$ on the original mass fraction $\phi$.

TABLE I. Values of the physical parameters.

| $\mathbb{H}$ | $\mathbb{L}$ | $\omega$ | $\rho$ | $\eta_0$ |
|---|---|---|---|---|
| $1.0\times10^{-2}$ cm | 1.0 cm | $1.9\times10^{4}$ s$^{-1}$ | 1.0 g cm$^{-3}$ | $8.1\times10^{3}$ P |
| $D_0$ | $K$ | $\phi_{\text{in}}$ | $a$ | $b$ |
| $7.8\times10^{-12}$cm$^2$ s$^{-1}$ | $5.5\times10^{-3}$ cm s$^{-1}$ | 0.9 | $5.0\times10^{-2}$ | $5.0\times10^{-2}$ |

For the rest of the paper we consider only the one-dimensional problem. This means we consider the case of uniform thickness of the liquid layer across the substrate, i.e., the free boundary $h$ is independent of $r$. In addition we assume that $\phi$ does not vary in the radial direction. We note that the assumption of a uniform thickness over the entire region is quite good except for neglecting variations with radius of the mass transfer rate to the surrounding gas, $k$.

For the thin liquid layer we make use of the fact that $\varepsilon_\ell \ll 1$ (and also that the reduced Reynolds number $(2\rho^2\omega^2H^4)/(\eta_0\ \exp(-\phi_{\text{in}}/(2b)))$ is small). We refer to the reviews by Refs. 37 and 38 and references therein for the derivation and discussion of lubrication approximation, modeling thin film dynamics in various fields of application. In the standard way, the leading order lubrication approximation renders the pressure to be independent of $z$, so that integrating the radial component of the momentum equation twice with respect to $z$, using the leading order boundary conditions of tangential stress $\partial_z u=0$ and normal stress $p=0$ at the free boundary $z=h(t)$, and the no-slip $u=0$ and impermeability condition $w=0$ at the solid substrate $z=0$ one obtains the expression,

$$u(r,z,t)=\int_0^z r(h(t)-z)\,e^{\varrho\phi}\,dz\,.$$

Using the continuity equation and integrating with respect to $z$ we obtain

$$w(z,t)=-\int_0^z (h(t)-q)(z-q)\,e^{\varrho\phi}\,dq, \tag{3a}$$

which couples to the diffusion equation

$$\partial_t\phi+w\partial_z\phi=\epsilon\,\partial_z\left(e^{\phi}\partial_z\phi\right), \tag{3b}$$

together with boundary conditions at $z=h(t)$

$$\frac{\epsilon}{\delta}e^{\phi}\partial_z\phi=-\frac{1}{\beta}(1+\gamma\phi)(1-\beta\phi), \tag{3c}$$

$$\partial_t h-w=-\delta(1+\gamma\phi), \tag{3d}$$

the boundary conditions at $z=0$

$$\partial_z\phi=0 \tag{3e}$$

and the initial conditions

$$h(0)=1\quad\text{and}\quad\phi(z,0)=0. \tag{3f}$$

We note that such a system has been considered by Reisfeld *et al.*[23,24] but without the variability of the diffusivity or viscosity.

The resulting nondimensional parameters in the problem for $w(z,t)$, $\phi(z,t)$, and $h(t)$ defined by Eqs. (3a)-(3f) are given by

$$\epsilon=\frac{1}{\varepsilon_\ell \text{Pe}},\ \delta=\frac{k\phi_{\text{in}}}{\varepsilon_\ell\mathbb{U}},\quad\text{where}\quad \text{Pe}=\frac{\mathbb{U}\mathbb{H}}{D_0 e^{\phi_{\text{in}}/2a}}, \tag{4a}$$

$$\gamma=\frac{2a}{\phi_{\text{in}}},\quad \beta=\frac{2a}{1-\phi_{\text{in}}}\quad\text{and}\quad \varrho=\frac{a}{b}\,. \tag{4b}$$

Typical values for the constants, that are involved in the spin coating process are given, e.g., in Bornside *et al.*[22] and Kreith *el al.*,[18] see Table I. We note that in particular Bornside *et al.* suggest that the viscosity and diffusivity change by five to six orders of magnitude as the solvent mass fraction increases from zero to one. This suggest a similar sensitivity for both properties with an approximate value for $a$ and $b$ as stated in the table. The nondimensional parameters corresponding to the data in the table are

$$\epsilon_{\text{ref}}=3.5\times10^{-7},\quad \delta_{\text{ref}}=1.1\times10^{-4},\quad \beta_{\text{ref}}=1.0,$$
$$\gamma_{\text{ref}}=0.1,\quad \varrho_{\text{ref}}=1.0.$$

For the analysis presented here, we will vary these parameters as we present our asymptotic analysis, but always assume that $\epsilon\ll1$, $\delta\ll1$, $\gamma\ll1$ and that $\beta$ and $\varrho$ are typically of order one. The relative size of $\varepsilon$ and $\delta$ will be changed as we consider different asymptotic regimes.

We note that numerical solutions to this problem can readily be generated. Here, our aim is to find analytical expressions for the solutions by considering physically relevant limiting cases of the nondimensional parameters and hence gain insight into the range of values that give particular behaviour such as skin formation.

## IV. ASYMPTOTIC REGIMES

The behaviour of the mixture layer is different depending on the relative size of $\delta$ and $\epsilon$. We present the behaviour for three different regimes, starting from small evaporation rates, as this turns out the richest case and conclude with the regime for large evaporation rates.

### A. Small evaporation ($\delta\ll\epsilon^{3/4}\ll1$)

#### 1. Short time scale ($t=O(1)$)

We start by considering the behaviour for $t=O(1)$. In this regime the layer thins due to fluid flow alone and the solution has one behaviour in the bulk and another in a small diffusive boundary layer adjacent to the free surface.

*a. Behaviour in the bulk.* Taking the lowest order problem we find

$$\partial_t \phi + w\,\partial_z \phi = 0\,, \tag{5a}$$

$$w = -\int_0^z (z-q)(h(t)-q) e^{\varrho\phi(q,t)}\,dq\,, \tag{5b}$$

$$\partial_t h - w = 0 \quad \text{at} \quad z = h\,, \tag{5c}$$

$$h = 1 \quad \text{and} \quad \phi = 0 \quad \text{at} \quad t = 0\,. \tag{5d}$$

This has the solution

$$\phi = 0\,, \text{ so that } w(z,t) = -\frac{hz^2}{2} + \frac{z^3}{6}. \tag{6}$$

Using this in the condition (5c) at $z = h$ we obtain

$$\partial_t h + \frac{h^3}{3} = 0 \text{ and hence } h(t) = \frac{1}{\sqrt{1+2t/3}}\,. \tag{7}$$

This solution is well known but note that care needs to be taken in getting this solution as (5b) contains an integral over the whole region including the boundary layer and (5c) is imposed in the boundary layer, however, so long as the integrand never gets large in the boundary layer, which will be true in the limit here, this solution is correct to lowest order.

*b. Behaviour in the diffusion boundary layer.* The boundary layer scalings are

$$z = h(t) + \epsilon^{1/2}\overline{z} \quad \text{and} \quad \phi(z,t) = \frac{\delta}{\epsilon^{1/2}}\,\overline{\phi}(\hat{z},t) \tag{8}$$

and note, for small evaporation, this corresponds to $\phi$ remaining small in this region. The problem in the boundary layer is then

$$\partial_t \overline{\phi} - \frac{h^2\overline{z}}{2}\,\partial_{\overline{z}}\overline{\phi} = \partial_{\overline{z}\overline{z}}\overline{\phi}\,, \tag{9a}$$

$$\partial_{\overline{z}}\overline{\phi} = -\frac{1}{\beta} \quad \text{at} \quad \overline{z} = 0, \tag{9b}$$

$$\overline{\phi} \to 0 \quad \text{as} \quad \overline{z} \to -\infty\,, \tag{9c}$$

$$\overline{\phi} = 0 \quad \text{at} \quad t = 0\,. \tag{9d}$$

We note that, because of the form of $h(t)$ in Eq. (7), after an initial transient to account for the initial condition, this problem has self-similar behaviour of the form,

$$\hat{\phi} = \frac{1}{\beta}\left(1+\frac{2}{3}t\right)^{1/2} u(\zeta), \quad \hat{z} = -\left(1+\frac{2}{3}t\right)^{1/2}\zeta \tag{10}$$

described by the boundary value problem

$$\frac{d^2u}{d\zeta^2} = \frac{1}{3}\,u - \frac{5}{6}\,\zeta\frac{du}{d\zeta}\,, \tag{11a}$$

$$\frac{du}{d\zeta}(0) = 1\,, \tag{11b}$$

$$u \to 0 \quad \text{as} \quad \eta \to \infty\,. \tag{11c}$$

The solution to Eq. (11) can be written in terms of Kummer's functions

$$M(a,b,z) := \frac{\Gamma(b)}{\Gamma(a)\Gamma(b-a)}\int_0^1 e^{zx}x^{a-1}(1-x)^{b-a-1}\,dx\,,$$

$$U(a,b,z) := \frac{1}{\Gamma(a)}\int_0^\infty e^{-zx}x^{a-1}(1+x)^{b-a-1}\,dx\,,$$

and is given by

$$u(\zeta) = \left[1 - \kappa\frac{2}{5}\,U\left(\frac{6}{5},\frac{3}{2},0\right) + 2\kappa\,U\left(\frac{1}{5},\frac{3}{2},0\right)\right] \times e^{5/12\,\zeta^2} M\left(\frac{6}{5},\frac{3}{2},\frac{5}{12}\zeta^2\right)\zeta + \kappa\,e^{5/12\,\eta^2} U\left(\frac{6}{5},\frac{3}{2},\frac{5}{12}\zeta^2\right)\zeta\,. \tag{12}$$

The value of $\kappa$ is determined by matching to the outer solution as $\zeta \to \infty$. Numerically, we determined the value up to six digits of accuracy and found $\kappa = -0.366172$.

To show the range of validity of this asymptotic solution, we compare it to the solution of the full model (3) in Figure 2. The latter was obtained numerically using a fully implicit Euler finite difference scheme on a fixed but non-uniform grid (this method was also used in the later figures whenever a time dependent problem needed to be solved numerically). We see that the two solutions agree very well for $t = O(1)$ but that the asymptotic approximation breaks down for longer times, which therefore need further treatment in Sec. II.

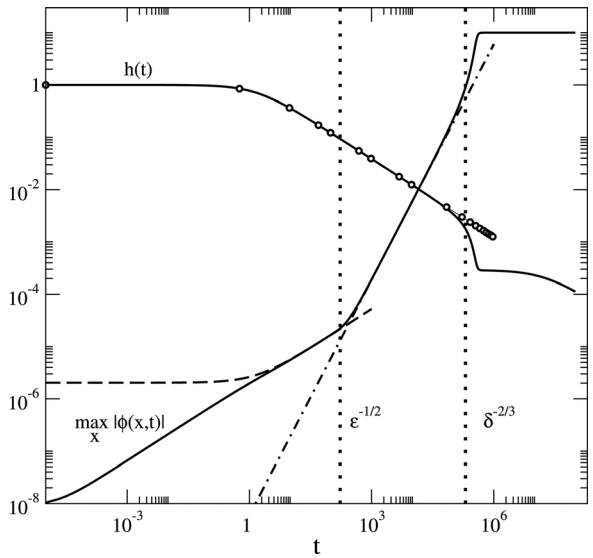


FIG. 2. Comparison of the numerical and asymptotic results in the small evaporation regime, for $\epsilon = 3.5 \times 10^{-5}$, $\delta = 1.1 \times 10^{-8}$, and for constant viscosity $\varrho = 0$. The solid curves denote the numerical results for $h(t)$ and $\max_x|\phi(x,t)|$ for Eq. (3). The dashed line shows $\max_x|\phi(x,t)|$ for the self-similar solution (10), (11), to the early time asymptotic problem; the behaviour for $h$, given by Eq. (7), is indicated by circles. The dash-dotted curves show the longtime approximations (16) for $\max_x|\phi(x,t)|$ for the leading order asymptotic solution in the medium time regime; note that in this regime, the leading order solution for $h(t)$ coincides with the long time expansion of Eq. (7), so we do not include a separate line. The two vertical dotted lines correspond to the times $t = \epsilon^{-1/2} = 169$ and $t = \delta^{-2/3} = 2.02 \times 10^5$, respectively.

### 2. Medium time scale $(t = O(\epsilon^{-1/2}))$

The previous results have established that as $t$ gets larger the layer thins according to $h = O(t^{-1/2})$ (from (7)), and using Eq. (10), a boundary layer forms of thickness $O((\epsilon t)^{1/2})$ in which the mass fraction is of size $\phi = O(\delta(t/\epsilon)^{1/2})$. There are several scenarios how this solution ceases to be valid as time progresses. The possibilities are

(a) Evaporation eventually becomes important: Since $\partial_t h$ and $w$ at $z = h$ decrease according to $O(t^{-3/2})$, they are of the same order as the term on the right hand side of Eq. (3d) when $t^{-3/2} = O(\delta)$, i.e., on the time scale $t_a = O(\delta^{-2/3})$.
(b) The thickness of the boundary layer grows to the size of the entire layer, i.e., when $h = O((\epsilon t)^{1/2})$. This occurs on the time scale $t_b = O(\epsilon^{-1/2})$.
(c) Thirdly, the mass fraction $\phi$ increases to be $O(1)$ in the boundary layer, resulting in formation of a skin with significant variations in the diffusive and the viscosity. This occurs when $\delta(t/\epsilon)^{1/2} = O(1)$, i.e., if $t_c = O(\epsilon/\delta^2)$.

We note that there is one distinguished limit, where all three time scales, $t_a$, $t_b$, and $t_c$ are equal. This happens when $\delta \sim \epsilon^{3/4}$. In the case when $\delta \gg \epsilon^{3/4}$, which we will refer to as *medium evaporation*, the time scales are ordered according to $t_c \ll t_a \ll t_b$ and, therefore, skin formation occurs first. In the other case, when $\delta \ll \epsilon^{3/4}$, which we call *small evaporation*, the time scales are ordered according to $t_b \ll t_a \ll t_c$. We now study the small evaporation case and determine the behaviour on the timescale of $t = t_b = O(\epsilon^{-1/2})$. Since $h = O(t^{-1/2})$ for large $t$, this shows that we should consider $h = O(\epsilon^{1/4})$ and $\phi = O(\delta(t_b/\epsilon)^{1/2}) = \delta\epsilon^{-3/4} \ll 1$. From the kinematic condition, (3d), we then find that $w = O(\epsilon^{3/4})$. Hence, we introduce the following scales for this regime:

$$t = \epsilon^{-1/2} t^*, \quad h = \epsilon^{1/4} h^*, \quad z = \epsilon^{1/4} z^*, \quad \omega = \epsilon^{3/4} \omega^*, \quad \phi = \frac{\delta}{\epsilon^{3/4}} \phi^*$$

and obtain the problem

$$\partial_{t^*} \phi^* + w^* \partial_{z^*} \phi^* = \partial_{z^* z^*} \phi^*, \tag{13a}$$

$$w^* = -\frac{h^* z^{*2}}{2} + \frac{z^{*3}}{6}, \tag{13b}$$

with boundary conditions at $z^* = h^*$

$$\partial_{z^*} \phi^* = -\frac{1}{\beta}, \tag{13c}$$

$$\partial_{t^*} h^* - w^* = 0, \tag{13d}$$

and at $z^* = 0$

$$\frac{\partial \phi^*}{\partial z^*} = 0. \tag{13e}$$

As $t^* \to 0$ we require

$$\phi^* \to 0 \quad \text{and} \quad h^* \to (2t^*/3)^{-1/2}, \tag{13f}$$

where the final conditions come from matching.

To examine when the solution to Eqs. (13)–(13f) may cease to be valid it is instructive to consider the long-time limit of the problem. For this limit it is convenient to set

$$z^* = \frac{1}{\sqrt{2/3t^*}} \xi, \qquad h^* = \frac{1}{\sqrt{2/3t^*}} f, \qquad \phi^*(z^*, t^*) = \psi(\xi, t^*). \tag{14}$$

Then, we obtain the problem

$$\frac{3}{2}\frac{1}{t^*}\partial_{t^*}\psi + \frac{3}{4}\frac{1}{t^{*2}}\xi\left(1 - \frac{3}{2}f\xi + \frac{1}{2}\xi^2\right)\partial_\xi \psi = \partial_{\xi\xi}\psi, \tag{15a}$$

with boundary conditions at $\xi = f$

$$\left(\frac{2}{3}t^*\right)^{1/2} \partial_\xi \psi = -\frac{1}{\beta}, \tag{15b}$$

$$\frac{2}{3}t^* \partial_{t^*} f - \frac{1}{3}f + \frac{1}{3}f^3 = 0, \tag{15c}$$

and at $\xi = 0$

$$\partial_\xi \psi = 0. \tag{15d}$$

This problem has the solution

$$f(t^*) = \frac{1}{\sqrt{1 + c_1/t^*}} \quad \text{and} \tag{16a}$$

$$\psi(\xi, t^*) = -\frac{1}{\beta}\left(\frac{2}{3}t^*\right)^{3/2} + \left(-\frac{\sqrt{3}}{2\sqrt{2}}\frac{1}{\beta}\xi^2 + c_2\right)t^{*-1/2} + \cdots \tag{16b}$$

for $t^* \gg 1$ and compares well with our numerical solution, see Figure 2.

The solution breaks down either when the evaporation becomes important for the evolution of the layer thickness $h$ or when the mass fraction $\phi$ becomes $O(1)$. From Eqs. (14) and (16), we obtain $\phi = O(\delta t^{3/2})$, and this becomes $O(1)$ when $t = O(\delta^{-2/3})$. Similarly, we find $h = O(t^{-1/2})$ thus $h_t = O(h^3) = O(t^{-3/2})$ and this will be of the same $O(\delta)$ as the evaporation when $t = O(\delta^{-2/3})$. This too yields $t = O(\delta^{-2/3})$ for the breakdown of validity, marking the transition to a new time regime.

### 3. Long time scale $(t = O(\delta^{-2/3}))$

For this new time regime, we therefore scale

$$t = \delta^{-2/3}\check{t}, \quad h = \delta^{1/3}\check{h}, \quad w = \delta\check{w}, \quad \phi = \check{\phi}.$$

Substitution into Eq. (3) yields the problem

$$\partial_{\check{t}}\check{\phi} + \check{w}\,\partial_{\check{z}}\check{\phi} = \frac{\epsilon}{\delta^{4/3}}\partial_{\check{z}}(e^{\check{\phi}}\partial_{\check{z}}\check{\phi}), \tag{17a}$$

$$\check{w} = \int_0^{\check{z}} (\check{z} - \check{q})(\check{h} - \check{q}) e^{\check{q}\check{\phi}}\, d\check{q}, \tag{17b}$$

with boundary conditions at $\check{z} = \check{h}$

$$\frac{\epsilon}{\delta^{4/3}} e^{\check{\phi}} \partial_{\check{z}}\check{\phi} = -\frac{1}{\beta}(1 + \gamma\check{\phi})(1 - \beta\check{\phi}), \tag{17c}$$

$$\partial_{\check{t}}\check{h} - \check{w} = -(1+\gamma\check{\phi}), \tag{17d}$$

and at $\check{z} = \check{h}$

$$\partial_{\check{z}}\check{\phi} = 0. \tag{17e}$$

We let

$$\begin{aligned}\check{\phi} &= \check{\phi}_0 + \frac{\delta^{4/3}}{\epsilon}\check{\phi}_1 + \cdots,\\ \check{h} &= \check{h}_0 + \frac{\delta^{4/3}}{\epsilon}\check{h}_1 + \cdots,\\ \check{w} &= \check{w}_0 + \frac{\delta^{4/3}}{\epsilon}\check{w}_1 + \cdots,\end{aligned} \tag{18}$$

and obtain that $\check{\phi}_0$ depends only on $t$. Hence, at next order the problem is

$$\frac{d\check{\phi}_0}{d\check{t}} = -\frac{1}{\beta}\frac{(1+\gamma\check{\phi})(1-\beta\check{\phi}_0)}{\check{h}_0}, \tag{19a}$$

$$\frac{d\check{h}_0}{d\check{t}} = -\frac{1}{3}e^{\varrho\check{\phi}_0}\check{h}_0^3 - (1+\gamma\check{\phi}_0), \tag{19b}$$

$$\check{w}_0 = e^{\varrho\check{\phi}_0(t)}\left(-\frac{\check{h}_0\check{z}^2}{2} + \frac{\check{z}^3}{6}\right). \tag{19c}$$

The initial conditions for this system comes from matching back with the medium time layer,

$$\phi_0 \to 0, \quad h_0 \sim (2t/3)^{-1/2} \quad \text{for} \quad t \to 0. \tag{19d}$$

The solution to this problem is obtained numerically and shown in Figure 3, where it is compared to the solution for the full lubrication model (3). As $t \to \infty$, the solution for $h_0$ and $\phi_0$ tends monotonically to the equilibrium $h_0 = 0$, $\phi_0 = -1/\gamma$ of the ODE system (19a) and (19b). The solutions are in excellent agreement even in the later stages of the medium time regime and throughout the late time regime. This is true if the diffusion remains strong enough to keep the mass fraction profile constant throughout the film, even as the exponential term on the right hand side of Eq. (17a) becomes smaller as $\phi_0$ approaches $-1/\gamma$. This is the case if the condition $\exp(1/\gamma) \ll \epsilon/\delta^{4/3}$ (or equivalently the very small evaporation limit $\delta \ll \exp(-3/(4\gamma))\epsilon^{3/4}$) is satisfied, which imposes a lower bound for $\gamma$ in order that no skin forms. For the values for $\varepsilon$ and $\delta$ chosen in Figure 3, this bound is about $\gamma = 1/\ln(\epsilon/\delta^{4/3}) = 0.07$. Note our choice of $\gamma$ is larger and indeed we found that the numerical solutions of Eq. (3) have flat mass fraction profiles. We have tested this bound by carrying out further simulations of Eq. (3) with smaller values of $\gamma$ but all other parameters unchanged. Already for $\gamma = 0.05$, the mass fraction profiles varied significantly across the film in the time period where $\phi$ increased rapidly towards the equilibrium value, and this effect became more pronounced for smaller $\gamma$; for $\gamma = 0.035$, the variation was more than 50%. We conclude that our estimate of the bound that defines very small evaporation is reasonably accurate.

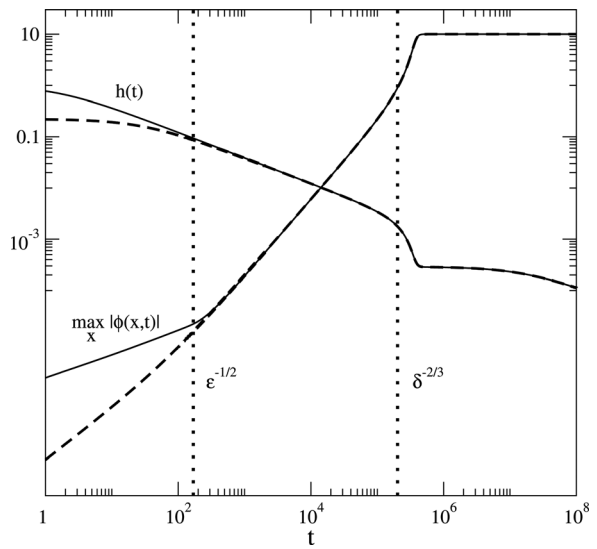


FIG. 3. Comparison of the numerical and asymptotic results in the small evaporation regime, for $\epsilon = 3.5 \times 10^{-5}$, $\delta = 1.1 \times 10^{-8}$, and for constant viscosity $\varrho = 0$. The solid curves denote the numerical results for $h(t)$ and $\max_x|\phi(x,t)|$ for Eq. (3). The dashed lines show the numerical for the leading order asymptotic problem in the late time regime (19). The two vertical dotted lines correspond to the times $t = \epsilon^{-1/2} = 169$ and $t = \delta^{-2/3} = 2.02 \times 10^5$, respectively.

### 4. The effect of mass fraction dependent viscosity

So far, all the figures only show results for the case where $\varrho = 0$, i.e., the viscosity does not depend on the mass fraction of the solvent. Indeed, setting $\varrho = 1$ hardly changes the evolution the film thickness and the maximum value of $\phi(x,t)$, with one notable exception. Once a significant amount of solvent has evaporated throughout the film (i.e., $\phi$ approaches $-1/\gamma$ everywhere rather than only in a thin boundary layer) the thinning due to centrifugal forces slows down dramatically as the viscosity in the bulk increases significantly. In fact, when we compare the evolution of $h(t)$ for the two choices of $\varrho$ in Fig. 4, the two lines only disagree after $t = O(\delta^{-2/3})$, where the effect of evaporation on the evolution of $h$ becomes significant. For $\varrho = 0$, thinning returns to $h \sim (2t/3)^{-1/2}$ after a while; for $\varrho = 1$ the thinning is slower and eventually becomes $h \sim (2\exp(-1/\gamma)/3t)^{-1/2}$. This behaviour follows from Eq. (19b) since $\check{\phi}_0 \to -1/\gamma$ as $\check{t} \to \infty$.

Note that, for $\max_x|\phi(x,t)|$, the results for the two values of $\varrho$ are indistinguishable in the figure. Also note that for the other cases, i.e., medium and large evaporation, the effect of replacing $\varrho = 0$ by $\varrho = 1$ is qualitatively the same for the full model, in the sense that in the numerical solution $\max_x|\phi(x,t)|$ is largely unaffected and only the final long time behaviour of $h(t)$ changes from $h \sim (2/3t)^{-1/2}$ to $h \sim (2\exp(-1/\gamma)/3t)^{-1/2}$.

Physically having the viscosity change only manifests itself when the concentration of solvent changes sufficiently from its initial value to significantly alter the viscosity. For large and medium evaporation rates this only occurs in a thin surface skin layer. In this layer the shear stress is very small, due to the proximity of the surface and so the viscosity changes have no appreciable effect on the behaviour. For

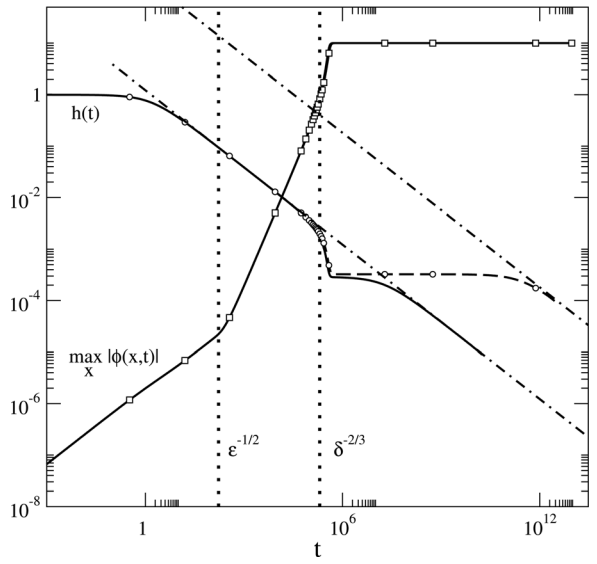


FIG. 4. Comparison of the numerical solution of Eq. (3) for $\varrho = 0$ (solid lines) with the results for $\varrho = 1$ (dashed lines with symbols). The dot-dashed lines indicate the long time behaviour for $h$ according to (19), which is $h \sim (2/3t)^{-1/2}$ for $\varrho = 0$ (bottom line) and $h \sim (2\exp(-1/\gamma)/3t)^{-1/2}$ for $\varrho = 1$ (top line).

small and very small evaporation rates the spatial uniformity of the concentration implies that the viscosity changes simply slow the thinning down and alter the velocities in a uniform manner. We do note that the increased viscosity may result in elongation stresses becoming significant in the layer, however, for the one dimensional model studied here we have neglected such effects. For these reasons in the analysis of the remaining cases in this paper, we focus exclusively on $\varrho = 0$.

### B. Medium evaporation $\left(\epsilon^{3/4} \ll \delta \ll \epsilon^{1/2} \ll 1\right)$

#### 1. Short time scale ($t = O(1)$)

For $t = O(1)$, we obtain the same results as in the short time regime for small evaporation. In particular we note that the analysis of the boundary layer is valid provided $\delta \ll \epsilon^{1/2}$. However, the transition to the next time regime occurs via the third scenario *c*) listed in Sec. IV A 2, since for $\delta \gg \epsilon^{3/4}$, the time scale $t_c = O\left(\epsilon/\delta^2\right)$ is the shortest of the three.

#### 2. Medium time scale $\left(t = O\left(\epsilon/\delta^2\right)\right)$

Using the earlier results we know that there is a boundary layer in which the concentration is expected to start to alter significantly. Hence, in the outer layer we take these scalings

$$t = \frac{\epsilon}{\delta^2}\breve{t}, \quad h = \frac{\delta}{\epsilon^{1/2}}\breve{h}, \quad z = \frac{\delta}{\epsilon^{1/2}}\breve{z},$$
$$\phi = \breve{\phi}, \quad w = \left(\frac{\delta}{\epsilon^{1/2}}\right)^3 \breve{w}. \tag{20}$$

This yields the problem

$$\partial_{\breve{t}}\breve{\phi} + \breve{w}\,\partial_{\breve{z}}\breve{\phi} = \frac{\epsilon^3}{\delta^4}\partial_{\breve{z}}\left(e^{\breve{\phi}}\partial_{\breve{z}}\breve{\phi}\right), \tag{21a}$$

$$\breve{w} = -\frac{\breve{h}\breve{z}^2}{2} + \frac{\breve{z}^3}{6}, \tag{21b}$$

with boundary conditions at $\breve{z} = \breve{h}$

$$\frac{\epsilon^{3/2}}{\delta^2}e^{\breve{\phi}}\partial_{\breve{z}}\breve{\phi} = -\frac{1}{\beta}(1+\gamma\breve{\phi})(1-\beta\breve{\phi}), \tag{21c}$$

$$\partial_{\breve{t}}\breve{h} - \breve{w} = -\frac{\epsilon^{3/2}}{\delta^2}(1+\gamma\breve{\phi}), \tag{21d}$$

and at $\breve{z} = 0$

$$\partial_{\breve{z}}\breve{\phi} = 0. \tag{21e}$$

As $\breve{t} \to 0$ we have

$$\breve{\phi} = 0 \quad \text{and} \quad \breve{h} = \left(\frac{2}{3}\breve{t}\right)^{-1/2}. \tag{21f}$$

For the regime, we are considering we know that $\epsilon^{3/2}/\delta^2 \ll 1$, thus to leading order we obtain an outer problem whose solution can readily be found to be

$$\breve{\phi} = 0 \quad \text{and} \quad \breve{h} = \left(\frac{2}{3}\breve{t}\right)^{-1/2}. \tag{22}$$

In the boundary layer we introduce the scalings

$$\breve{z} = \breve{h} + \frac{\epsilon^{3/2}}{\delta^2}\bar{\bar{z}}, \quad \breve{\phi} = \bar{\bar{\phi}}, \quad \breve{t} = \bar{\bar{t}}. \tag{23}$$

This leads to the leading order inner problem

$$\partial_{\bar{\bar{t}}}\bar{\bar{\phi}} + \left(1 + \gamma\bar{\bar{\phi}}(0) - \frac{3\bar{\bar{z}}}{4\bar{\bar{t}}}\right)\partial_{\bar{\bar{z}}}\bar{\bar{\phi}} = \partial_{\bar{\bar{z}}}\left(e^{\bar{\bar{\phi}}}\partial_{\bar{\bar{z}}}\bar{\bar{\phi}}\right), \tag{24a}$$

with the boundary condition at $\bar{\bar{z}} = 0$

$$e^{\bar{\bar{\phi}}}\partial_{\bar{\bar{z}}}\bar{\bar{\phi}} = -\frac{1}{\beta}(1+\gamma\bar{\bar{\phi}})(1-\beta\bar{\bar{\phi}}). \tag{24b}$$

In addition, we require as $\bar{\bar{z}} \to -\infty$ that

$$\bar{\bar{\phi}} \to 0, \tag{24c}$$

and as $\bar{\bar{t}} \to 0$

$$\bar{\bar{\phi}} \to 0. \tag{24d}$$

As time increases the analysis breaks down when either the boundary layer thickness equals the thickness $h$ of the film or evaporation begins to significantly modify the evolution of $h$. In fact, we expect that the time scale for both events must be the same: If $\phi$ is order one in the boundary layer, then evaporation has a leading order effect on the film thickness exactly when the boundary layer thickness is no longer small compared to $h$ itself. From a diffusion balance in Eq. (24a), we find that the boundary layer grows like $\epsilon^{1/2}t^{1/2}$; from Eq. (22), we obtain $h = O(t^{-1/2})$. Equating the two yields $t = O(\epsilon^{-1/2})$. On this time scale $h_t = O\left(\epsilon^{3/4}\right)$; this does not

seem to balance evaporation, i.e., the right hand side of Eq. (3d), which appears to be $O(\delta) \gg \epsilon^{3/4}$. However, we have to take into account that $\phi(h)$ is already very close to $-1/\gamma$ so that $(1+\gamma\phi(h)) = O(\epsilon^{3/4}/\delta)$.

### 3. Long time scale $(t = O(\epsilon^{-1/2}))$

In this time regime, we scale according to

$$t = \epsilon^{-1/2}\tilde{t}, \quad h = \epsilon^{1/4}\tilde{h}, \quad z = \epsilon^{1/4}\tilde{z}, \\ \phi = \tilde{\phi}, \quad w = \epsilon^{3/4}\tilde{w}. \tag{25}$$

Note that here we do not have a boundary layer, i.e., there is only one spatial scaling. Introducing these scalings yields the problem

$$\partial_{\tilde{t}}\tilde{\phi} + \tilde{w}\,\partial_{\tilde{z}}\tilde{\phi} = \partial_{\tilde{z}}\left(e^{\tilde{\phi}}\partial_{\tilde{z}}\tilde{\phi}\right), \tag{26a}$$

$$\tilde{w} = -\frac{\tilde{h}\tilde{z}^2}{2} + \frac{\tilde{z}^3}{6}, \tag{26b}$$

with boundary conditions at $\tilde{z} = \tilde{h}$

$$\frac{\epsilon^{3/4}}{\delta}e^{\tilde{\phi}}\partial_{\tilde{z}}\tilde{\phi} = -\frac{1}{\beta}(1+\gamma\tilde{\phi})(1-\beta\tilde{\phi}), \tag{26c}$$

$$\frac{\epsilon^{3/4}}{\delta}\left(\partial_{\tilde{t}}\tilde{h} - \tilde{w}\right) = -(1+\gamma\tilde{\phi}), \tag{26d}$$

at $\tilde{z} = 0$

$$\partial_{\tilde{z}}\tilde{\phi} = 0. \tag{26e}$$

and as $\tilde{t} \to 0$

$$\tilde{\phi} \to 0 \quad \text{and} \quad \tilde{h} \to (2\tilde{t}/3)^{-1/2}. \tag{26f}$$

We let

$$\tilde{\phi} = \tilde{\phi}_0 + \frac{\epsilon^{3/4}}{\delta}\tilde{\phi}_1 + \cdots, \\ \tilde{h} = \tilde{h}_0 + \frac{\epsilon^{3/4}}{\delta}\tilde{h}_1 + \cdots, \\ \tilde{w} = \tilde{w}_0 + \frac{\epsilon^{3/4}}{\delta}\tilde{w}_1 + \cdots, \tag{27}$$

and obtain to leading order the problem

$$\partial_{\tilde{t}}\tilde{\phi}_0 + \tilde{w}_0\,\partial_{\tilde{z}}\tilde{\phi}_0 = \partial_{\tilde{z}}\left(e^{\tilde{\phi}_0}\partial_{\tilde{z}}\tilde{\phi}_0\right), \tag{28a}$$

$$\tilde{w}_0 = -\frac{\tilde{h}_0\tilde{z}^2}{2} + \frac{\tilde{z}^3}{6}, \tag{28b}$$

where the boundary condition at $\tilde{z} = \tilde{h}_0$ is now given by

$$\tilde{\phi}_0 = -\frac{1}{\gamma}, \tag{28c}$$

and at $\tilde{z} = 0$

$$\partial_{\tilde{z}}\tilde{\phi}_0 = 0. \tag{28d}$$

As $\tilde{t} \to 0$

$$\tilde{\phi}_0 \to 0, \qquad \tilde{h}_0 \to (2\tilde{t}/3)^{-1/2}. \tag{28e}$$

Note that the two boundary conditions at $z = \tilde{h}$, (26c) and (26d), result in a single leading order condition at $z = \tilde{h}_0$, (28c). To close the problem, we need an additional condition, which comes from carrying out the expansion for Eqs. (26c) and (26d) to next order. We obtain

$$e^{\tilde{\phi}_0}\partial_{\tilde{z}}\tilde{\phi}_0 = -\frac{\gamma}{\beta}(\gamma\tilde{\phi}_{0\tilde{z}} + \gamma\tilde{\phi}_1)(1-\beta\tilde{\phi}_0), \tag{29a}$$

and the boundary condition at $z = \tilde{h}_0$

$$\partial_{\tilde{t}}\tilde{h}_0 - \tilde{w}_0 = -(\gamma\tilde{\phi}_{0\tilde{z}} + \gamma\tilde{\phi}_1). \tag{29b}$$

From this we obtain by elimination of $\tilde{\phi}_1(\tilde{h}_0)$ the following condition at $z = \tilde{h}_0$

$$\partial_{\tilde{t}}\tilde{h}_0 - \tilde{w}_0 = \frac{\beta\gamma}{\beta+\gamma}e^{-1/\gamma}\partial_{\tilde{z}}\tilde{\phi}_0. \tag{30}$$

The solution of the leading order problem (28) is shown in Figure 5 (dashed-dotted line for $\tilde{h}_0$ and square symbols for $\tilde{\phi}_0$). In order to capture the small bump shown in the expanded view in Figure 6 (top) for $\max_x|\phi|$, higher order corrections to the leading order asymptotic results are required. In practice, the solution to Eq. (28) will change on a very long time scale (long even in terms of $\tilde{t}$) due to the

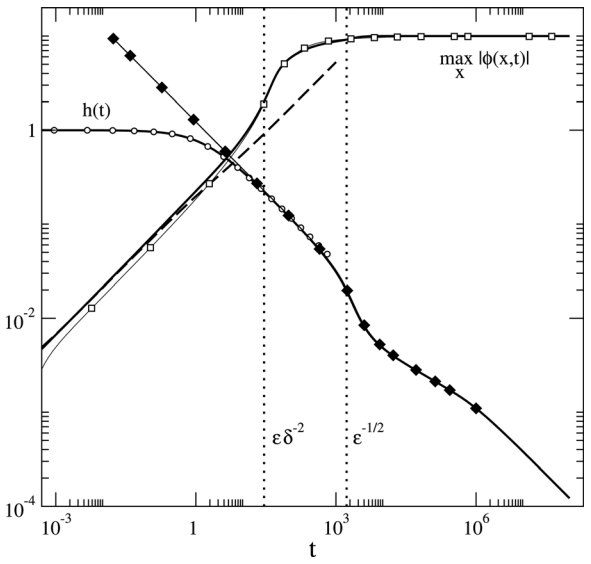


FIG. 5. Comparison of the numerical and asymptotic results in the medium evaporation regime, for $\epsilon = 3.5 \times 10^{-7}$, $\delta = 1.1 \times 10^{-4}$, and for constant viscosity $\varrho = 0$. The thick solid curves denote the numerical solutions of Eq. (3). The circles and the dashed line denote the results for the asymptotic approximations in the short time regime (7) and (9) (circles for $h(t)$ and the dashed line for $\max_x|\phi(x,t)|$). The solution for $h(t)$ remains valid to leading order in the medium time regime (see Eq. (22)), while the solution of the leading order inner problem (24) for $\max_x|\phi(x,t)|$ in this time regime is given by squares; it continues to agree well with the solution of (3) also in the long-time regime. The thin line with the solid diamonds corresponds to the solution for $h(t)$ to the leading order asymptotic problem (28), (30) in the long time regime. The two vertical dotted lines indicate the times $t = \epsilon/\delta^2 = 28.9$ and $t = \epsilon^{-1/2} = 1.69 \times 10^3$, respectively.

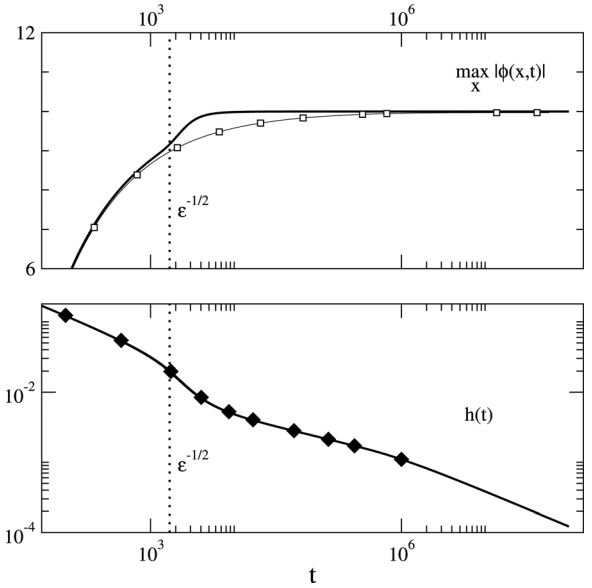


FIG. 6. Expanded details of the graphs given in Fig. 5 for $\max_x|\phi(x,t)|$ and $h(t)$. All parameters, line styles and symbols identical to Fig. 5.

small values of $\gamma$. This is an interesting problem, which we shall not pursue further here.

### C. Large evaporation $(\epsilon^{1/2} \ll \delta \ll 1)$

#### 1. Short time scale $(t = O(\epsilon/\delta^2))$

We anticipate a thin boundary layer will be created by the evaporation at the surface. Appropriate variables in the boundary layers are

$$z = h(t) + \frac{\epsilon}{\delta}\hat{z} \quad \text{and} \quad \phi(z,t) = \hat{\phi}(\hat{z},t)\,. \tag{31}$$

This scaling allows for order one values of $\phi$ in the boundary layer and balances the terms on the left and right hand side of Eq. (3c). Balancing the time derivative in the bulk with the diffusion requires that we rescale time by

$$t = \frac{\epsilon}{\delta^2}\hat{t}, \tag{32}$$

which implies a short time regime (since $\epsilon/\delta^2 \ll 1$). With these scalings, the leading order boundary layer problem becomes

$$\partial_{\hat{t}}\hat{\phi} + \left(1 + \gamma\hat{\phi}(0)\right)\partial_{\hat{z}}\hat{\phi} = \partial_{\hat{z}}\left(e^{\hat{\phi}}\partial_{\hat{z}}\hat{\phi}\right), \tag{33a}$$

with the boundary condition

$$e^{\hat{\phi}}\partial_{\hat{z}}\hat{\phi} = -\frac{1}{\beta}(1+\gamma\hat{\phi})(1-\beta\hat{\phi}) \quad \text{at} \quad \hat{z} = 0. \tag{33b}$$

A far-field condition at $z \to -\infty$ comes from matching to the outer problem. On the short time scale (32), the leading order outer problem becomes trivial; it has the constant solution $h = 1$ and $\phi = 0$. Matching yields

$$\hat{\phi} \to 0 \quad \text{as} \quad \hat{z} \to -\infty\,. \tag{33c}$$

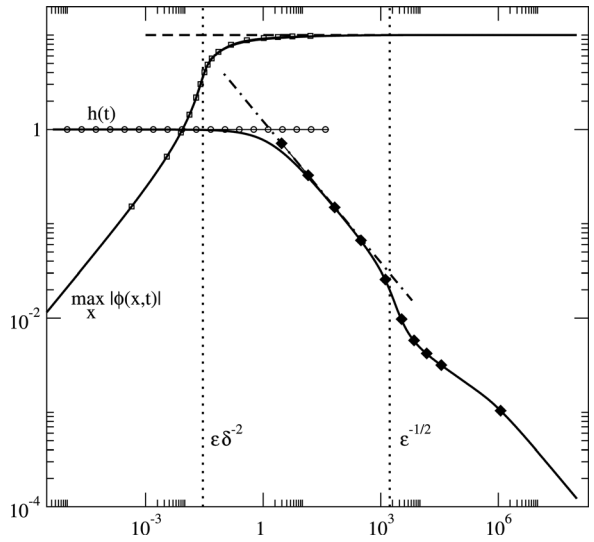


FIG. 7. Comparison of the numerical and asymptotic results in the large evaporation regime, for $\epsilon = 3.5 \times 10^{-7}$, $\delta = 3.48 \times 10^{-3}$, and for constant viscosity $\varrho = 0$. The solid curves denote the numerical solutions of Eq. (3). The thin lines with circles and the squares denote the results for the asymptotic problems in the short time regime (circles for $h(t)$, which is constant to one, and squares for $\max_x|\phi(x,t)|$, obtained from Eq. (33)). In the medium time regime, the solution for the asymptotic problems (34), (39) is given by a dash-dotted line for $h(t)$ and by a dashed line for $\max_x|\phi(x,t)| = 1/\gamma$. In the long time regime, the solution to Eqs. (28) and (30) is indicated by a thin line with solid diamonds for $h(t)$. The two vertical dotted lines correspond to the times $t = \epsilon/\delta^2 = 2.89 \times 10^{-2}$ and $t = \epsilon^{-1/2} = 1.69 \times 10^3$, respectively.

The solutions to the leading order asymptotic problems are compared to the solutions of the full model are compared in Fig. 7. The figure also contains lines for the solutions to the asymptotic problems in the medium and long time regime stated in the next two sections.

This time regime ends when $w$ and $h_t$ balance in Eq. (3d); since both $w$ and $h$ are $O(1)$, this happens when $t = O(1)$.

#### 2. Medium time scale $(t = O(1))$

Since also $h = O(1)$ also $w = O(1)$ for $z = O(1)$, we leave all variables in their original scaling in this regime. Hence, the leading order problem is directly obtained from problem (3) and has the solution

$$\phi_0 = 0, \qquad h_0 = \frac{1}{\sqrt{1+2t/3}}\,. \tag{34}$$

However, this solution does not satisfy the boundary condition (3c), so we need to introduce a boundary layer at $z = h(t)$.

*Boundary layer problem* Setting

$$z = h(t) + \epsilon^{1/2}z^* \tag{35}$$

the boundary problem reads

$$\partial_t\phi + \left(\frac{\delta}{\epsilon^{1/2}}(1+\gamma\phi(0)) - \frac{h^2 z^*}{2} + \epsilon\frac{z^{*3}}{6}\right)\partial_{z^*}\phi = \partial_{z^*}\left(e^{\phi}\partial_{z^*}\phi\right), \tag{36a}$$

at $z^*=0$

$$\frac{\epsilon^{1/2}}{\delta}e^{\phi}\partial_{z^*}\phi=-\frac{1}{\beta}(1+\gamma\phi)(1-\beta\phi), \tag{36b}$$

as $z^*\to-\infty$

$$\tilde{\phi}\to 0. \tag{36c}$$

We consider the expansions

$$\phi=\phi_0+\frac{\epsilon^{1/2}}{\delta}\phi_1+O(\epsilon/\delta^2),\quad h=h_0+\frac{\epsilon^{1/2}}{\delta}h_1+O(\epsilon/\delta^2) \tag{37}$$

and obtain

$$\phi_0(0)=-\frac{1}{\gamma},\quad \phi_1(0)=\frac{\beta\gamma}{\beta+\gamma}e^{-1/\gamma}\partial_{z^*}\phi_0(0)\,, \tag{38}$$

where the leading order problem is

$$\partial_t\phi_0-\left(\frac{\beta\gamma e^{-1/\gamma}}{\beta+\gamma}\partial_{z^*}\phi_0(0)+\frac{h_0^2z^*}{2}\right)\partial_{z^*}\phi_0=\partial_{z^*}\left(e^{\phi_0}\partial_{z^*}\phi_0\right), \tag{39a}$$

with the boundary condition for $\phi_1$ at $z^*=0$ given by (38). As $z^*\to-\infty$

$$\phi_0\to 0, \tag{39b}$$

and $\phi_0\to 0$ as $t\to 0$.

We note that as $t\to\infty$ then $h_0=O(t^{-1/2})$. Since the diffusion balance yields $z^*=O(t^{1/2})$ and the boundary layer grows to the size of the film thickness $O\left(\epsilon^{1/2}t^{1/2}\right)=O\left(t^{-1/2}\right)$ which suggests that the next time regime is $t=O\left(\epsilon^{-1/2}\right)$.

### 3. Long time scale $t=O\left(\epsilon^{-1/2}\right)$

For the long-time behaviour we obtain the same scales as in Eq. (25) in Sec. IV B 3. This results in the same set of equations as in that section.

## V. CONCLUSIONS

Our analysis of spin coating a polymer blended in a volatile solvent shows that in the high Peclet number regime, there are essentially three asymptotic regimes in our simplified model that describe distinct paths of the film thinning process starting from the initial liquid layer to the final solid film and can be described by corresponding asymptotic boundary value problems for the small, medium and large evaporation limits. They are distinguished by the relationship between three main parameters, the ratio of diffusion to advection $\epsilon$, the ratio of evaporation to advection $\delta$ and the ratio of the diffusivity of the pure polymer, and the initial mixture $\exp(-1/\gamma)$.

We show that, while the basic mechanisms discussed in detail by Bornside *et al.*[22] are valid, the important practical problem of understanding how to prevent the eventual skin formation can in fact be quantified. We predict that for the very small evaporation limit, when $\delta\ll\exp(-3/(4\gamma))\epsilon^{3/4}$ is satisfied, no skin formation will occur.

In the remaining small, medium, and large evaporation cases, where there is always skin formation, we show that the time scales at which the skin appears and the details of its formation are different. In the small evaporation regime, the solvent is initially depleted in a thin boundary layer region near the liquid surface. However, the boundary layer spreads out until it spans the entire film, after which the mass fraction profile flattens out across the film. If the evaporation is *very* small, this flat profile is maintained until all solvent is evaporated. But if it is not *very* small, the changes in diffusivity can give rise to steeper mass fraction gradients and eventually to skin formation.

In the medium evaporation regime, an order one change of the mass fraction occurs within the surface boundary layer, giving rise to a skin within a medium time scale. Underneath the skin, the polymer concentration is still at its initial value. After the skin has formed, depletion due to evaporation is slowed down because diffusion of the solvent through the boundary layer is greatly diminished. However, there are still significant mass fraction gradients so the volume profile continues to evolve, albeit on a very slow time scale. These gradients are driven by the fact that the material at surface is almost pure polymer.

The large evaporation regime is qualitatively similar to the medium evaporation case, except that the skin arises on a very fast timescale, i.e., much smaller than order one, before any liquid has been ejected due to the centrifugal forces.

The behaviour described above is characteristic for liquids of constant viscosity as well as for concentration dependent viscosity. In fact our numerical results are almost indistinguishable during the time regime when evaporation is still dominant. A dramatic quantitative change sets in after significant amounts of the solvent has evaporated throughout the film and the thinning for the liquid with concentration dependent viscosity slows down considerably. We note, however, that we have restricted our investigations to the case where the viscosity changes with the polymer mass fraction at the same rate as the diffusivity. However, even in Bornside *et al.*'s data[22] it is apparent that as the polymer fraction is raised from 1% to 10%, the viscosity changes dramatically compared to the diffusivity; only for even larger polymer concentrations the viscosity increases more slowly. This rapid change suggests using a $\rho$ that is significantly larger than one, and it would certainly interesting to extend our analysis to include this regime as well. Alternatively, one could use a different constitutive law that better fits the dependence of the viscosity over a wider range of concentrations, e.g., the law used by Bornside *et al.*

For practical purposes, we note that for a given material the parameter $\epsilon$ can be modified by a reasonable amount by changing the spinning speed of the disk or modified dramatically by the initial mass fraction of the solvent, while $\delta$ can be modified reasonably either by changing the spinning speed and changing the overlying solvent mass fraction, whereas $\exp(-1/\gamma)$ depends very sensitively on both the initial mass fraction of the solvent and the overlying solvent mass fraction.

We note that the theory we construct in this paper assumes that the film is flat, i.e., independent of the radial (and axial) variables from the beginning. Even though this condition can be achieved by an appropriate experimental setup, it is not the typical situation. Rather, the liquid mixture is usually deposited in the middle of the disk when it is started up. As Emslie *et al.*[4] have shown for the case without evaporation, the centrifugal forces flatten out the film; this happens on the time scale used here to nondimensionalise the equations. Hence, the film becomes flat in general for $t \gg 1$. For small and medium evaporation, this happens before any skin forms and the asymptotic regimes with $t \gg 1$ remain valid. However, for larger evaporation, the skin appears before the film has completely flattened so that the final outcome is likely to be different from the situation described in this paper.

There will be further aspects to consider in the future that have not been explored in detail previously in the literature or in this paper. Initially they will concern the possible formation of instabilities of the flow in higher dimensions. Extending the number of constituents of the polymer blends will introduce new phenomena such as phase separation or liquid-liquid dewetting.

## ACKNOWLEDGMENTS

The authors gratefully acknowledge the generous support of OCCAM (Oxford Centre for Collaborative Applied Mathematics) under support supplied by Award No. KUK-C1-013-04, made by the King Abdullah University of Science and Technology (KAUST). C.P.P. and B.W. are especially grateful for the support and hospitality during their OCCAM Visiting Fellowships. The authors also enjoyed lively and very fruitful discussions with Professor John R. Ockendon and Dr. Chris J.W. Breward.

[1]C.-C. Changa, C.-L. Paia, W.-C. Chena, and S. A. Jenekheb, "Spin coating of conjugated polymers for electronic and optoelectronic applications," Thin Solid Films **479**, 254 (2005).
[2]P. Jukes, S. Heriot, J. Sharp, and R. Jones, "Time-resolved light scattering studies of phase separation in thin film semiconducting polymer blends during spin-coating," Macromolecules **38**, 2030 (2005).
[3]J.-S. Kim, P. K. H. Ho, C. E. Murphy, and R. H. Friend, "Phase separation in polyfluorene-based conjugated polymer blends: Lateral and vertical analysis of blend spin-cast thin films," Macromolecules **37**, 2861 (2004).
[4]A. G. Emslie, F. T. Bonner, and L. G. Peck, "Flow of a viscous liquid on a rotating disk," J. Appl. Phys. **29**, 858 (1958).
[5]J. A. Moriarty, L. W. Schwartz, and E. O. Tuck, "Unsteady spreading of thin liquid films with small surface tension," Phys. Fluids A **3**, 733 (1991).
[6]I. S. McKinley, S. K. Wilson, and B. R. Duffy, "Spin coating and air-jet blowing of thin viscous drops," Phys. Fluids **11**, 30 (1999).
[7]S. K. Wilson, R. Hunt, and B. R. Duffy, "The rate of spreading in spin coating," J. Fluid Mech. **413**, 65 (2000).
[8]T. G. Myers and J. P. F. Charpin, "The effect of the Coriolis force on axisymmetric rotating thin film flows," Int. J. Non-Linear Mech. **36**, 629 (2001).
[9]I. S. McKinley and S. K. Wilson, "The linear stability of a drop of fluid during spin coating or subject to a jet of air," Phys. Fluids **14**, 133 (2002).
[10]L. W. Schwartz and R. V. Roy, "Theoretical and numerical results for spin coating of viscous liquids," Phys. Fluids **16**, 569 (2004).
[11]A. Acrivos, M. J. Shah, and E. E. Petersen, "On the flow of a non-Newtonian liquid on a rotating disk," J. Appl. Phys. **31**, 963 (1960).
[12]C. J. Lawrence and W. Zhou, "Spin coating of non-Newtonian fluids," J. Non-Newtonian Fluid Mech. **39**, 137 (1991).
[13]M. A. Spaid and G. M. Homsy, "Viscoelastic free surface flows: spin coating and dynamic contact lines," J. Non-Newtonian Fluid Mech. **55**, 249 (1994).
[14]M. A. Spaid and G. M. Homsy, "Stability of viscoelastic dynamic contact lines: An experimental study," Phys. Fluids **9**, 823 (1997).
[15]J. Charpin, M. Lombe, and T. Myers, "Spin coating of non-Newtonian fluids with a moving front," Phys. Rev. E **76**, 016312 (2007).
[16]T. J. Rehg and B. G. Higgins, "Spin coating of colloidal suspensions," AIChE J. **38**, 489 (1992).
[17]B. S. Dandapat, B. Santra, and A. Kitamura, "Thermal effects on film development during spin coating," Phys. Fluids **17**, 062102 (2005).
[18]F. Kreith, J. H. Taylor, and J. P. Chong, "Heat and mass transfer from a rotating disk," J. Heat Transfer **81**, 95 (1959).
[19]D. P. B. III and M. Manley, "Combined flow and evaporation of fluid on a spinning disk," Phys. Fluids **9**, 870 (1997).
[20]A. Meyerhofer, "Characteristics of resist films produced by spinning," J. Appl. Phys. **49**, 3993 (1978).
[21]P. C. Sukanek, "Spin coating," J. Imaging Technol. **11**, 184 (1985).
[22]D. Bornside, C. Macosko, and L. Scriven, "Spin coating: One-dimensional model," J. Appl. Phys. **66**, 5185 (1989).
[23]B. Reisfeld, S. G. Bankoff, and S. H. Davis, "The dynamics and stability of thin liquid films during spin coating. I. Films with constant rates of evaporation or absorption," J. Appl. Phys. **70**, 5258 (1991).
[24]B. Reisfeld, S. G. Bankoff, and S. H. Davis, "The dynamics and stability of thin liquid films during spin coating. II. Films with unit-order and large Peclet numbers," J. Appl. Phys. **70**, 5267 (1991).
[25]S. D. Howison, J. A. Moriarty, J. R. Ockendon, E. L. Terrill, and S. K. Wilson, "A mathematical model for drying paint layers," J. Eng. Math. **32**, 377 (1997).
[26]B. V. de Fliert and R. V. der Hout, "Stress-driven diffusion in a drying liquid paint layer," Eur. J. Appl. Math. **9**, 447 (1998).
[27]M. H. Eres, D. E. Weidner, and L. W. Schwartz, "Three-dimensional direct numerical simulation of surface-tension-gradient effects on the leveling of an evaporating multicomponent fluid," Langmuir **15**, 1859 (1999).
[28]B. V. de Fliert and R. V. der Hout, "A generalized Stefan problem in a diffusion model with evaporation," SIAM J. Appl. Math., **60**, 1128 (2000).
[29]P. L. Evans, L. W. Schwartz, and R. V. Roy, "A mathematical model for crater defect formation in a drying paint layer," J. Colloid Interface Sci. **227**, 191 (2000).
[30]L. W. Schwartz, R. V. Roy, R. R. Eley, and S. Petrash, "Dewetting patterns in a drying liquid film," J. Colloid Interface Sci. **234**, 363 (2001).
[31]P. Gaskell, P. Jimack, M. Sellier, and H. Thompson, "Flow of evaporating, gravity-driven thin liquid films over topography," Phys. Fluids **18**, 1 (2006).
[32]C. J. Lawrence, "The mechanics of spin coating of polymer films," Phys. Fluids **31**, 2786 (1988).
[33]C. J. Lawrence, "Spin coating with slow evaporation," Phys. Fluids A **2**, 453 (1990).
[34]P. de Gennes, "Solvent evaporation of spin cast films: crust effects," Eur. Phys. J. E **7**, 31 (2002).
[35]T. Okuzono, K. Ozawa, and M. Doi, "Simple model of skin formation caused by solvent evaporation in polymer solutions," Phys. Rev. Lett. **97**, 136103 (2006).
[36]D. E. Bornside, R. A. Brown, P. W. Ackmann, J. R. Frank, A. A. Tryba, and F. T. Geyling, "The effects of gas phase convection on mass transfer in spin coating," J. Appl. Phys. **73**, 585 (1993).
[37]A. Oron, S. H. Davis, and S. G. Bankoff, "Long-scale evolution of thin liquid films," Rev. Mod. Phys. **69**, 931 (1997).
[38]R. V. Craster and O. K. Matar, "Dynamics and stability of thin liquid films," Rev. Mod. Phys. **81**, 1131 (2009).